CLM - R 165

CLM - R 165

UKAEA

Report

REVERSAL OF THE TOROIDAL MAGNETIC FIELD IN PINCHES

E P BUTT
L FIRTH
R F GRIBBLE
LI YIN AN
A A NEWTON
A J L VERHAGE

CULHAM LABORATORY
Abingdon Oxfordshire

1977

Available from H. M. Stationery Office

C/18

£1.00

CLM-R 165

REVERSAL OF THE TOROIDAL MAGNETIC FIELD IN PINCHES

E P Butt, L Firth, R F Gribble[o], Li Yin An[+], A A Newton and A J L Verhage

Culham Laboratory, Abingdon, Oxon, OX14 3DB, UK
(Euratom/UKAEA Fusion Association)

Summary

Developments in the understanding of the reversed field pinch as a relaxed state having a near minimum magnetic energy content are reviewed. Experimental results from ZETA and HBTX I show that plasmas tend to relax towards the above state, and self-reversal of the toroidal field is observed. The self reversal phenomenon has also been investigated on FRSX and a 3.5 m linear pinch having the same parameters. Results from all these experiments are reviewed and discussed.

[o]On attachment from Los Alamos Scientific Laboratory, USA

[+]On attachment from the Institute of Physics, Chinese Academy of Sciences, Peking, The People's Republic of China.

May 1977

SBN 85311 ~~0514~~
-671-9

1. INTRODUCTION

The phenomenon of self reversal by which a "stabilised pinch" generates, through turbulence and instability, an external reversed field is widely observed. It occurs in experiments in which the plasma is surrounded by a real or equivalent flux conserving shell provided the pinch parameter*, θ, exceeds some critical value. A significant theoretical advance was made recently (TAYLOR, 1974) when it was shown that, if dissipation is allowed a "stabilised pinch" configuration will relax to a minimum energy state, which for a range of values of θ, typical of those found experimentally, is a reversed field configuration. Thus a reversed field configuration is the natural final state.

Under certain conditions a high degree of stability is obtained when the toroidal field is reversed, with a much reduced level of magnetic fluctuation (BUTT ET AL, 1965). In these cases, observed on ZETA, it has been shown that the conditions for ideal MHD stability are satisfied (ROBINSON and KING, 1968).

In this paper observations made on three widely different experiments, viz ZETA, HBTX and FRSX, are described. Field reversal is seen in each when the conditions of the theory are satisfied. Furthermore the reversal is maintained when the current pulse is prolonged by a power crowbar showing the reversal mechanism to be strong. Additional results are obtained from a linear experiment with the same parameters as FRSX.

---

* Here we define $\theta = B_{\theta WALL}/\bar{B}_z$ or $2\pi r_{WALL}\ I/\Phi_z$ where $\Phi_z = 2\pi\int_o^{r_{WALL}} B_z\, rdr$. Where I is the current, Φ_z the toroidal field and r_{WALL} the plasma wall radius.

2. FIELD CONFIGURATION

2.1 The $\beta = 0$ Model

Taylor (TAYLOR, 1974) has shown that the pinch configuration will relax to a minimum energy state whose nature depends on the ratio of the poloidal to toroidal fluxes. Conditions are for practical purposes characterised by θ and when the final value is in the range of $1.20 < \theta < 1.56$ the external B_z is reversed and there is cylindrical symmetry. This result, which is for pressureless plasma (i.e. $\beta = 0$), has field distributions of the Bessel Function Model (BFM), i.e. $B_z = B_o J_o(\mu r)$ and $B_\theta = B_o J_1(\mu r)$ where $\mu = 2\theta$.

At $\theta \approx 1.56$ helical equilibria are predicted with a fixed wavenumber and an amplitude increasing with applied toroidal field E_z. The onset of these states coincides approximately with violation of the MHD stability criterion for the total range of magnetic pitch ($P(r) = rB_z(r)/B_\theta(r)$) across the plasma minor radius i.e. $P_{WALL} > -3P_{AXIS}$ (ROBINSON, 1971).

The above results, which are obtained for infinite straight cylindrical geometry, apply with some small corrections to a torus. However when θ is small and comparable to or less than the aspect ratio r_{WALL}/R_{MAJOR} (where R_{MAJOR} is the toroidal radius) a toroidally dominated situation occurs which may be applicable to Tokamak. The transition occurs when $q \gtrsim 0.8$ (q is the safety factor $\dfrac{r_{WALL}B_z(r)}{R_{MAJOR}B_\theta(r)}$).

It is interesting to note that in the pinch the relaxation process leads to a maximum pitch on axis, i.e. the pitch falls with increasing radius. A vacuum field region (i.e. zero conductivity) necessarily exists due to physical separation between the plasma and shell (or coils) where $P(r) \propto r^2$

so that plasma and outer magnetic field configurations can only match with no minimum in the pitch (a necessary condition for ideal MHD stability in the pinch) when the outer toroidal field is reversed. In contrast in Tokamak the relaxed condition should give a uniform pitch (i.e. q) although a minimum on axis is usually observed with the radial distribution matching the outer vacuum region without an off axis minimum.

2.2 Effect of Finite Beta

The above theory is for $\beta = 0$ so that although the final minimum energy state contains appreciable shear it confines no pressure. Since the energy dissipated during the relaxation process (assumed to be lost for $\beta = 0$) is sufficient to generate a high beta, the model can reasonably be extended to accommodate pressure up to the limit permitted by Suydam's Criterion (SUYDAM, 1958) to give the High Beta Model (HBM). This has been done using a relaxation technique which adiabatically expands the Taylor configuration to maintain pressure balance (NEWTON ET AL,1975). In these cases as θ is increased the beta rises and $\beta \sim 0.075\ \theta^3$ (other models give similar results e.g. GOWERS et al, 1976). The distributions generated not only satisfy all the simplified MHD stability criteria such as no magnetic pitch minimum, limited range of pitch variation, etc (summarised in Table 1) but are rigorously MHD stable. Helical formations can be expected at large values of θ which are not described by the HBM. These were also predicted with a sharp boundary model (YEH,1973) and show a limited range of wave number ($kr_{WALL} \sim 1.0$ to 1.33).

The magnitude of reversed axial field at wall $F(=\pi r^2_{WALL} B_{zWALL}/\phi_z$, the reversal ratio) given by both models is shown in Fig. 1a. Corresponding BFM and HBM configurations lie on a line passing through the origin because they

both have the same P_{WALL} which is proportional to F/θ. Field configurations of BFM and HBM are shown in Figs. 1b and 1c.

2.3 Other Models

A number of detailed models have been worked out which are based on currents (j_z, j_θ) maintained by particular distributions of electric fields E_z and E_θ through the simplified Ohm's law. They are variants or extensions of the FFPM (Force Free Paramagnetic Model (BICKERTON, 1958)) which is also shown in Fig. 1. In this type of model the conductivity anisotropy (i.e. ratio of $\sigma_\perp/\sigma_\parallel$) and the radial dependence of $\sigma_\parallel$ and the electric fields are used as free parameters. In this way some of the features either observed in experiment (i.e. small pressure gradient and small current density near the wall) or required in theoretical studies to ensure stability (i.e. a reduction in j_z near the axis) can be generated. Other variants based on assumed P(r) with pressure gradient related to the Suydam limiting value are frequently used. Two examples of this type (ROBINSON, 1971 and ROBINSON, 1969) are shown in Fig. 2.

2.4 General

These models map out a broad region in the F,θ plane where plasma can be expected to find a low energy state (see Fig. 1). Its approximate left hand boundary is the BFM where $\beta = 0$. As β is raised the state is shifted towards the HBM. Moving upwards from the HBM, i.e. as F is reduced, we approach the FFPM in which only a low beta is permitted. As θ is increased and large reversals are generated the cylindrically symmetric configurations give way to helices (not covered by the HBM numerical model). The modified FFPM configurations have been shown to be stable to resistive MHD with $\beta_{AXIS} \sim 0.27$, $\theta \sim 2.0$ (BUTT et al, 1974); stability to ideal MHD is possible at slightly higher values (ROBINSON, 1971).

3. EXPERIMENTS

In the theory it has been assumed that the plasma vessel (wall) and the rigid magnetic boundary (shell) coincide. In experiment these two are separate and also the effective radii at which the azimuthal and axial fluxes are conserved may be outside the shell.

A variety of measurements on ZETA give best consistency in level of magnetic fluctuations over a range of conditions if θ is calculated at the liner* rather than the shell. The former value calculated at peak current is usually quoted. Consequently values of θ and F at the wall (i.e. liner or quartz tube inside radius) have been used here when presenting experimental results.

3.1 Parameters

Parameters of the experiments discussed here are summarised in Table 2. In ZETA (BURTON ET AL, 1961) the toroidal field is applied with a 1s rise time and for the duration of the 5 ms current pulse ϕ_z is trapped inside a 3 cm thick aluminium casing. The metal walled liner, which is a vacuum vessel containing the plasma, has 0.5 ms time constant, is close to the casing.

On HBTX the toroidal field is applied before the start of current and reversal can be driven during or after the rise of the pulse. This "fast programming" (GOWERS ET AL, 1972) is used to generate a range of field configurations (before the onset of instabilities) and stable RFP are produced in this way. The quartz vessel permits this rapid field change which occurs in a few microseconds. The current pulse then decays when passive crowbars are used on both circuits. Alternatively the toroidal field can be crowbarred before the current rise trapping the flux inside the shell.

On FRSX a flux conserving shell is used and the current rise time, although much faster than on ZETA is not sufficient for the programmed formation of the pinch as on HBTX. However a power crowbar is available to extend the pulse at constant current for 50 μs.

The 3.5 m linear experiment has similar parameters to FRSX. (Details are given by BUTT ET AL, 1975). The axial field is given by a capacitor circuit

---

*In experimental publications on ZETA this quantity was θ_1 and θ referred to $B_{\theta\ WALL}/B_{zo}$ where B_{zo} was the initial axial field.

with a diode crowbar switch feeding a multiturn coil and a "square wave" of plasma current is driven by a 7 element transmission line between electrodes. This facility is used for studies with plasma conditions identical to those of FRSX but in open ended geometry.

3.2 FRSX

Figure 3 shows waveforms of the normal FRSX discharge operating in the overswing (i.e. uncrowbarred) mode which show the features characteristic of the self reversing discharge. As the I rises the Φ_z also increases and B_z at the wall decreases as expected from the paramagnetic effect. Then a discontinuity is seen in B_{zWALL} which falls to nearly zero when a second discontinuity leads rapidly to reversal. These are accompanied by indentations in I and characteristic steps in Φ_z.

Since the axial flux signal is measured between the vessel and the shell the flux within the discharge vessel must be calculated using B_{zWALL} to obtain θ and F. The resulting curve in Fig. 4 shows reversal occuring by progression through a series of states which lie initially to the right of the HBM. By peak current a quasi stationary position between HBM and BFM is attained and when the capacitor bank overswing reduces the current the trajectory returns to the left of the BFM in a region characteristic of reversed toroidal currents in the outer regions of the plasma.

When the current is sustained by a power crowbar the reversal persists while the current (and θ) remain high. However $B_{z\ wall}$ and Φ_z show relaxation oscillations in which a decay of the reversal is followed by an abrupt regeneration (see Fig. 5). The corresponding F - θ plot (see Fig. 6) shows the trajectory of relaxation being approximately orthogonal to the HBM production and crossing it and the BFM. At later times when the current decays the trajectory follows a course similar to that in the overswing mode.

A set of three sine/cosine wound Rogowski coils placed 6.7 and 13.4 cm apart were used to search for m = 1 perturbations. At the onset of the discharge

a toroidal drift motion outwards to 0.5 cm was clearly seen. During the growth of self reversal this drift was reversed and in this and subsequent phases irregular displacements of the plasma by $\sim$ 0.5 cm and rarely exceeding 1 cm were observed. Although the coils were monitored simultaneously on a number of occasions and perturbations detected no fixed or clearly defined wavelengths could be determined.

In conditions of low magnetic field, when operating in the overswing mode, $B_{z\ wall}$ does not return to its initial value B_{zo} when the current reaches zero and the end of a half cycle. The F - θ trajectory exhibits a hysteresis which is clearly visible by a failure to return to F=1 at the end of the first half cycle of current and measured by H(=1-F(θ=0)) which is shown in Fig.7. Thus at the end of the half cycle plasma remains close to the wall with the toroidal field intensified on axis and no total axial current. Estimates suggest a low plasma temperature of $\lesssim$ 2 eV at this time with pressure balance maintained by the walls.

3.3 HBTX

On this device self reversal is observed in a number of "stabilsed z-pinches" (SZP) and is always preceded by instability. Forced reversals can also be generated by driving the axial field through zero while the plasma current is rising to give "reversed field pinches" (RFP).

Examples of SZP are shown in Figs. 8 and 9. With a peak current $\hat{I}$ = 75 kA (Fig. 8) the plasma is formed by 4 µs with $\theta \sim 2.2$ and $B_{z\ wall}$ positive. Then an instability occurs and the plasma relaxes within 1 µs to a helix with λ = 45 cm and a large self reversal. The helix and reversal decay until 20 µs when a second but weaker relaxation occurs but no reversal is generated in this case. With 100 kA peak current (Fig. 9) similar behaviour is seen. However, the self reversal is larger and the helix of shorter wavelength $\sim$ 30 cm. Shortly after the m = 0 mode has also been seen in both cases. When RFP are generated by fast programming it is possible to arrive close to stable conditions. Figure 10 shows that the most stable case (ROBINSON ET AL, 1972) is formed with $\theta \sim 2$ and F $\sim$ - 0.5; it diffuses at a classical rate to F = 0 at $\sim$ 20 µs with θ increasing.

At higher currents, e.g. $\hat{I}$ = 75 kA RFP shown in Fig. 11, programmed formation drives θ to 3.75 and it relaxes quickly to the region of the HBM where it remains for $\sim$ 8 μs. Diffusive processes raise θ and F until at 30 μs there is another, but weaker, relaxation which marginally enhances the reversal.

In some conditions it is still possible to keep θ below 2 at high peak currents. Figure 12 shows an example which remains near the HBM for $\sim$ 20 μs when the absolute level of current and reversal decay together. At later times θ increases until a relaxation at $\sim$ 40 μs is seen. The later time behaviour is influenced by the large reservoir of reversed axial flux outside the tube which is present because of the stray circuit inductance causing Φ_z to decay faster than I_z and θ to rise. When the current has fallen to $\sim$ 10 kA a high $\theta \sim 2.5$ to 3.5 remains without further self reversal. In these conditions the plasma temperature estimated from codes and pressure balance is $\lesssim$ 2 eV.

Magnetic field distributions found by probes inserted in the plasma show broadly the HBM pattern but modified for low current density near the wall. At currents 40 to 160 kA the distributions several μs after formation are insensitive to the method of formation (VERHAGE and ROBINSON, 1976). An example at $\hat{I} \sim 75$ kA is shown in Figure 13. At higher currents persistent and fluctuating detail structure is seen superimposed on the radial distributions.

In summary we note that on HBTX it is possible to form discharges over a wide range of conditions (viz initial F, θ) by fast programming. These are then seen to relax to near the same final state, sometimes violently when the plasma is set up with far from optimum values of F,θ.

More examples of self reversal and the tendency of θ, when driven to high values initial values $\sim$ 3 to 4, to relax to 1.8 to 2.0 are given in (BUTT ET AL, 1974) where curves of $\theta(t)$ presented show the tendency of θ to remain in the latter range during the (passive) crowbar phase of the discharge.

3.4 ZETA

Self reversal of the axial magnetic field was observed on ZETA and in

many cases this gave rise to a stable RFP (i.e. quiescence characterised by a much reduced level of fluctuation); The "Quiet Period" is described elsewhere (BUTT ET AL, 1965, ROBINSON ET AL, 1967 ROBINSON and KING, 1968).

Figure 14 shows measurements of F as a function of θ for a range of discharge conditions ; it can be seen that self reversal occurs for $\theta \gtrsim 1.25$. At low pressures (i.e. 0.5 mtorr) the resistance is anomalously high, giving a large power input to the plasma; in this instance the data lies towards the right of the HBM. Another set of data at 2.0 mtorr and peak current of 360 kA, recorded at the onset of quiescence, show states in the HBM/BFM region.

Magnetic probe measurements of the field configuration at $\hat{I} \sim 330$ kA and $p_o = 1.5$ mtorr (see Fig. 5, BUTT ET AL 1965) show reasonable agreement with the BFM. There are small discrepancies in the outer regions corresponding to $j_z > 0$ as expected for $E_z > 0$ rather than the reversed value of the BFM; also the structure in the outer regions changes just before and during quiescence for which $E_z < 0$ is required.

The evolution of a high current discharge is shown in Fig. 15 for $\hat{I} \sim$ 0.8 MA in which quiescence was obtained. The data points, taken at $\sim$ 0.2 ms intervals, show evolution to the right of the region until self reversal occurs when θ falls. Then the changes in θ and F occur more slowly until the reversal decays and the discharge returns to its starting point.

Cases have been observed with the self reversal lasting for $\sim$ 1 ms which was followed by a regeneration of self reversal of about the same duration (ROBINSON ET AL, 1967).

Helical formations were seen when $\theta \gtrsim 1.8$ and when $\theta \sim 2.1$ a strong helix with amplitude of about half the wall radius was found (LEES and RUSBRIDGE, 1959). The helix formation is associated with difficulty in raising the current beyond a certain level. This "current limitation" effect is accompanied by a large increase in volt seconds consumption and energy loss (BUTT and NEWTON, 1976).

Self reversal and quiescence are not observed in all conditions where $\theta > 1.5$ and a threshold level of initial pressure, p_o, and $\hat{I}^2/p_o$ the energy density must be exceeded (BUTT et al., 1965). At low pressures the discharge is resistive with anomaly factors of up to 3; in these cases the level of fluctuations remains high and reversal is not observed although helical structure is present.

3.5 Linear Pinch

Discharges between electrodes have been produced with 30 kA constant current pulses for 200 μs at conditions (p_o, r_w, $\hat{I}$) identical to those in FRSX. Typical oscillograms of I, Φ_z and $B_{z\ wall}$ are shown in Fig. 16 where transient reversal can be seen. The fluctuations in $B_{z\ WALL}$ are larger in amplitude than in FRSX by a factor of 5 and are comparable with the initial field (B_{zo}). Investigations with search coils showed the reversal to be localised with a correlation length less than the tube diameter. In this and all other situations examined there is no steady or sustained reversal as observed in the toroidal experiments.

The F - θ plot in Fig. 17 confirms the absence of sustained reversal and is significantly different from that obtained on FRSX (see Fig. 6) for identical plasma conditions. The region of fluctuations corresponds to a time average $F > 0$ where a higher θ is reached than in FRSX.

4. DISCUSSION

In all the toroidal experiments self reversal is observed when $\theta \gtrsim 1.4$ and the plasmas relax to a region in F - θ space near the BFM and HBM (except with low currents - see later). The observed field distributions are similar to those of the BFM the main difference being that the current density near the wall is much lower in experiment. When the current is prolonged to maintain θ the reversal persists. Relaxation oscillations occur with $\sim$ 10 μs period in FRSX, $\sim$ 1 ms on ZETA and these can be interpreted as reduction of the reversal by field diffusion followed by regeneration. The F - θ trajectory during these oscillations follows approximately the direction

of constant magnetic energy (GIMBLETT and WATKINS, 1975).

Certain values of magnetic energy per particle (given as $\hat{I}^2/p_o$ and particle line density (N) must also be exceeded. There are examples on all experiments (e.g. ZETA at low currents and pressures, HBTX in the later stage of the pulse) where reversal is not obtained even with $\theta \sim 2.5$ to 3.5. In these cases the plasma resistivity is thought to be so high that the azimuthal currents which might support the reversal are greatly reduced.

It is not clear which property best delineates the conditions for turbulent activity leading to reversal. For ZETA $\hat{I}^2/p_o$ was used but comparison with HBTX suggests that the nominal resistive time ($\tau_R = 4\pi r^2_{wall}/\eta$) should exceed the current pulse length. Also S ($=\tau_R/\tau_H$ where $\tau_H \sim r_{wall}/V_{A\theta}$ and $V_{A\theta}^2 = B_{\theta}^2{}_{wall}/4\pi\rho$) should exceed about 10^2. Estimates of these parameters for each experiment are given in Table 3 showing the range of S is roughly up to 10^5 for ZETA, to 10^4 for HBTX and up to 500 for FRSX.

In conditions where self reversal has occurred and θ is high, helical formations are also seen. In ZETA these occur when $\theta \gtrsim 1.8$ and in HBTX at comparable values. The threshold for helices is above that given by the BFM but is consistent with the trend expected when β is finite. It is notable that helical formations appear when the stability criterion based on the total range of pitch is violated. This criterion relates to higher θ and lower F if finite beta is included. The helices have wavenumbers corresponding to $ka \sim 2.0$ to 4.0 on HBTX and are somewhat different to the $ka = 1.25$ given by Taylor's theory. However their existence is brief with the current and θ decaying and the plasma reverting to the cylindrical state.

Finally, we note that toroidal effects if present are not strong. Waveforms of SZP in FRSX and HBTX in comparable conditions are closely similar and reproducible up to full self reversal. Since the aspect ratios differ by a factor of at least two we conclude that there is no significant toroidal influence on the reversal at large aspect ratio. However on ZETA during the current rise there is some evidence for m = 1, n = 4, 5 or m = 2, m = 7, 9, 11 toroidal resonances

(BURTON ET AL, 1961) but it is not clear what part they play in self reversal. The well documented ZETA RFP has a negligible helical component during the quiescent phase (ROBINSON and KING, 1968).

A strong geometrical effect is however shown by the linear experiment where a reversal cannot be sustained. Transient local reversal is observed during large amplitude fluctuations. Since the axial flux in this device returns through a region not filled with plasma and links an external conductor we infer that a topological constraint precludes a normal self reversal.

The results presented here show that reversal is associated with m = 1 and 0 modes in HBTX and higher order modes in ZETA. There are two well defined regimes depending on the ratio of current rise time, τ_I, to τ_H (BUTT ET AL, 1975). When $\tau_I \ll \tau_H$ a well compressed plasma is observed in which a strong m = 1 helix develops. Reversal follows from the break-up of this helix the detail of which is difficult to resolve in experiment. The mechanism is discussed elsewhere (VERHAGE and ROBINSON, 1975), and a detailed study has been made (VERHAGE ET AL, 1976, GOWERS ET AL, 1976). Note that the helical instability does not itself have reversed toroidal field and is quite different from the relaxed stable helical state (discussed earlier).

When $\tau_I \gg \tau_H$ the helical and other instability modes grow and saturate before the value of θ required for reversal is reached. This effect is observed on ZETA where high order radial modes (turbulence) are seen. The rising current takes the plasma gradually through a succession of quasi equilibria with reversal occurring as θ exceeds 1.5. Turbulent mechanisms of reversal have been discussed in terms of the cutting and rejoining of flux tubes in a "tangled discharge model" (RUSBRIDGE, 1976 and KADOMTSEV, 1976) or by the "dynamo" effect (GIMBLETT and WATKINS, 1975).

It is clear also that two competing processes are present, one leading to reversal (better stated as the generation and anomalous B_z i.e. non paramagnetic effect) and the other to its decay. In conditions of low S the decay dominates and reversal is not seen. When S is above some threshold $\sim 10^2$ reversal occurs and can be established for long times if S is much higher. When the geometrical

arrangement precludes reversal strong fluctuations are seen suggesting that the reversal mechanism is a strong process. The comparison of predictions with experimental results is summarised in Table 4.

5. CONCLUSIONS

The theoretical predictions indicate a region (in θ, F space) where the generation of reversed field configuration is favoured and, at higher θ, a region in which non-cylindrical formations occur. Results obtained from a variety of discharges fall in these regions. Relaxation occurs even when plasmas are formed impulsively with (θ, F) initially well away from this region. Helical configurations are found at high values of θ and their lifetime is found in experiment to be relatively shorter than that of the cylindrical discharges. The field configurations are close to but not in detailed agreement with theoretical predictions and the discrepancies can be expected when the applied electric fields and plasma properties near the boundaries are taken into account.

We conclude that there is general agreement with the theoretical predictions of plasma relaxation to reversed field configurations. Detailed differences can be understood when reasonable physical conditions are taken into account such as the effects of finite beta and low current density near the walls.

6. ACKNOWLEDGEMENTS

It is a pleasure to acknowledge discussions with J B Taylor and our other colleagues.

TABLE 1

SIMPLIFIED CRITERIA FOR IDEAL MHD STABILITY IN AN INFINITE CYLINDER

Magnetic Pitch $P = rB_z/B_\theta$

Axial flux inside the shell $\Phi_{zs} = 2\pi \int_0^{r_{SHELL}} B_z \, r dr$

1. Magnetic Modes.

   (a) No minimum in P

   (b) Limited range of pitch. $P_{WALL} > -{}^1/3 \, P_{AXIS}$

   (c) Wall stabilisation $\Phi_z > 0$

   } (ROBINSON, 1971)

2. Pressure Modes.

   (a) Suydams' Criterion $\nabla p > -\frac{rB_z^2}{32\pi}\left(\frac{P'}{P}\right)^2$ (SUYDAM, 1958)

   (b) Shear on axis $\alpha < -\left({}^4/9 + f(\beta)\right)$ where $f(\beta) > 0$ and $f(0) = 0$ (ROBINSON, 1972)

   (c) Integral criterion for $m = 1$, $\beta_\theta < 1$ (ROBINSON, 1971)

   (d) Integral criterion for $m = 0$, $\beta_\theta < \frac{1}{2} + \beta_R$ where β_R is local beta at the $B_z = 0$ surface. (BAKER and MANN, 1974)

TABLE 2

PARAMETERS OF EXPERIMENTS USED FOR SELF REVERSAL STUDIES

	Vessel Major/Minor Radii	Shell Radii	Peak Current	Pressure	Rise Time
ZETA	150/50 cm	53 cm	330 - 800 kA	1.7 - 3 mtorr	0.8 - 2.6 msec
HBTX	100/6 cm	7.5 cm	40 - 160 kA	13.5 - 40 mtorr	2 - 6 μsec
FRSX	32/4 cm	6 cm	30 - 70 kA	10 - 50 mtorr	15 μsec
3.5 m Pinch	350*/4 cm	5 cm	30 kA	∿ 40 mtorr	25 μsec

* straight tube; length quoted

TABLE 3

NOMINAL PROPERTIES OF RFP

	Minor radius cm	$\hat{I}$ MA	p_o mtorr	I^2/p_o	β_θ	τ_R sec	τ_H 10^{-6} sec	$S = \tau_R/\tau_H$	Rise time 10^{-6} sec	Pulse length Scale 10^{-6} sec
ZETA										
Low Current		.13	1.2	.014	.05	.001	6.6	170	1000	1000
Medium Current*	50	.42	2.0	.088	.1	.04	2.2	20,000	1200	3000
High Current		.80	2.7	.240	.1	.2	1.3	150,000	1500	5000
HBTX										
Low Current+		.012	40	3.6×10^{-6}	1	3.0×10^{-6}	4.9	0.5	3	40
Medium Current	6	.040	40	40×10^{-6}	.7	0.65×10^{-4}	1.5	50	3	40
High Current		.160	40	640×10^{-6}	.7	4.1×10^{-3}	0.4	10,000	6	40
FRSX										
Typical Current	4	.055	40	76×10^{-6}	.7	2.5×10^{-4}	.5	500	15	50

* Nominal minimum value for quiescence is 0.3 MA.

\+ Typical value of current at which reversal is lost by diffusion although θ remains high

TABLE 4 COMPARISON OF THEORETICAL PREDICTIONS AND EXPERIMENTAL RESULTS

Topic	Theory low beta	Theory high beta	Experiment - Fast $\tau_I \leq \tau_H$	Experiment - Slow $\tau_I >> \tau_H$
Onset of reversal of toroidal field	$\theta = 1.2$	$\theta = 1.4$	$\theta \geq 2$	$\theta \geq 1.4$
Onset of Helices	$\theta = 1.56$	$\theta \sim 2.4$	$\theta \geq 2$ θ reaches 4 transiently	$\theta \geq 1.8$
Wavelength of helix	$kr_{WALL} = 1.25$ amplitude increases with I_z/ϕ_z	$kr_{WALL} = 1.0 - 1.33$ and kr_{WALL} decreases with β on a Sharp boundary model	$kr_{WALL} \sim 2$ to 4 amplitude increases with θ	Wavelength not well defined in FRSX. In ZETA m=1 n=4,5 and m=2 n=7,9,11 giving $kr_{WALL} \sim 1.3$ to 1.7.
Resistive Effects	"Small but finite dissipation" is assumed.	Electric fields calculated to be monotonic with	$S_M = \tau_\eta/\tau_H \gtrsim 2 \times 10^2$ for reversal (Tested with S_M range 1 to 10^5)	
Mechanism of reversal	Not known	Model of Isotropic Turbulence gives $\gtrsim 2$ radial wavelengths	Well defined m = 1 helix precedes reversal also m = 0 radial expansion observed.	No. large amplitude m = 1 helix. 5-10 radial modes with $\frac{\delta B}{B} \sim 10^{-2}$ and long turbulent cells parallel to $\underline{B}$.
Reversed field Configuration and beta	BFM $\beta=0$ $\{B_\theta = B_o J_1(2\theta r)$, $B_z = B_o J_o(2\theta r)$	HBM similar to BFM with distribution of magnetic pitch displaced outwards. $\beta \propto \theta^3$	Sometimes resembles BFM with high order components. Superimposed. β_θ saturates at ~ 0.6 at late times.	Similar to BFM but $j \gtrsim 0$ near wall; $\beta_\theta \sim 0.05$. Weak higher order components have also been seen

REFERENCES

BAKER, D A and MAN, L W, Los Alamos Scientific Laboratory Report LA-5656-PR p 96 (1974)

BICKERTON, R J, Proc. Phys. Soc. 72, 618 (1958).

BURTON, W M et al. Proceedings of the 1st IAEA Conference on Plasma Physics and Controlled Nuclear Fusion, Salzburg, (1961). Nuclear Fusion Supp. (1962), pt 3, 903.

BUTT, E P et al. Proceedings of the 2nd IAEA Conference on Plasma Physics and Controlled Nuclear Fusion, Culham, (1965), paper CN-21/32, 2, 751.

BUTT, E P, et al. Proceedings of the 5th IAEA Conference on Plasma Physics and Controlled Nuclear Fusion, Tokyo, (1974) paper CN-33/E9-2.

BUTT, E P, and FIRTH, L, Pulsed High Beta Plasmas paper A3.10, Edited by D E Evans, Pergamon, Oxford, 1976.

BUTT, E P et al. Pulsed High Beta Plasmas, paper C2.1, Edited by D E Evans, Oxford, 1976.

BUTT, E P, et al. Proceedings of the 7th EPS Conference on Controlled Fusion and Plasma Physics, Lausanne, (1975).

BUTT, E P and NEWTON, A A. Pulsed High Beta Plasmas Paper C2.2. Edited by D E Evans, Pergamon, Oxford (1976).

GIMBLETT, C G and WATKINS, M L. Proceedings of the 7th EPS Conference on Controlled Fusion and Plasma Physics, Lausanne, (1975).

GOWERS, C W, Proceedings of the Second Topical Conference on Pulsed High Beta Plasmas, Garching, (1972), Institut fur Plasma Physik report IPP 1/127 paper A3.

GOWERS, C W et al. Proceedings of the 6th IAEA Conference on Plasma Physics and Controlled Nuclear Fusion, Berchtesgaden (1976) paper CN-35/E-2.

KADOMTSEV, B, Proceedings of the 6th IAEA Conference on Plasma Physics and Controlled Nuclear Fusion, Berchtesgaden (1976) paper CN-35/B1.

LEES, D J, RUSBRIDGE, M G, Proceedings of the 4th Int. Conference on Ionisation Phenomena in Gases, Uppsala, 2, (1959), 954.

NEWTON, A A, et al. Pulsed High Beta Plasmas, paper B2.6. Edited by D E Evans Pergamon, Oxford (1976).

ROBINSON, D C, and KING, R E. Proceedings of the 3rd IAEA Conference on Plasma Physics and Controlled Nuclear Fusion, Novosibirsk, (1968) paper CN-24/B-8.

ROBINSON, D C, Plasma Physics 13, (1971), 439.

ROBINSON, D C Plasma Physics 11, (1969), 893.

ROBINSON, D C et al. Proceedings of the 5th EPS Conference on Controlled Fusion and Plasma Physics, Grenoble, 1, (1972), 47.

ROBINSON, D C, BOLAND, B C, KING, R E and PEASE, R S, Abstracts of the 2nd EPS Conference on Controlled Fusion and Plasma Physics, Stockholm, (1967).

RUSBRIDGE, M G, Private Communication (1976).

SUYDAM, B R, Proceedings of 2nd U.N. Internat. Conference on Peaceful Uses of Atomic Energy, Geneva, 31, (1958), 165.

TAYLOR, J B, Phys. Rev. Lett. 33, (1974), 1139 and Proceedings of the 5th IAEA Conference on Plasma Physics and Controlled Nuclear Fusion, Tokyo, (1974), paper CN-33/PDN-1, also Pulsed High Beta Plasmas, paper B1.6 Edited by D E Evans, Pergamon, Oxford 1976.

VERHAGE, A J L and ROBINSON, D C, Pulsed High Beta Plasmas paper B1.5 Edited by D E Evans, Pergamon, Oxford (1976).

VERHAGE A J L, FURZER, A S and ROBINSON, D C Culham Laboratory Preprint CLM P463. (1976).

YEH, T, Phys. of Fluids, 16, (1973), 516.

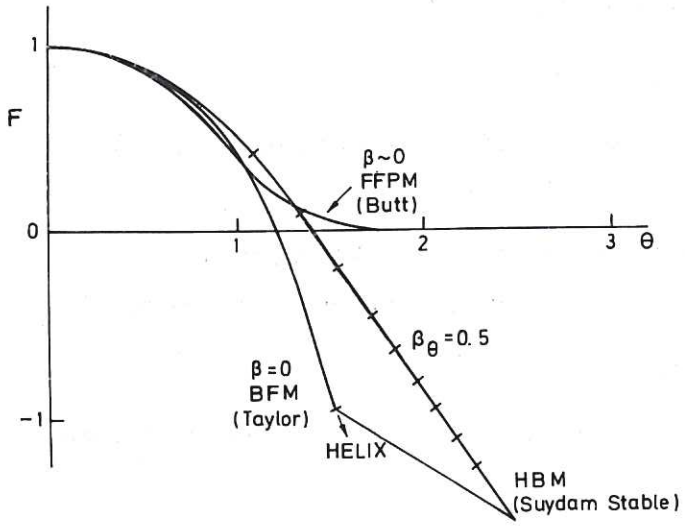

Fig.1a Toroidal field reversal ratio, F, vs pinch parameter θ for Bessel function (BFM), High beta (HBM) and Force free paramagnetic (FFPM) model pinch configurations. The bars on HBM show β_θ increasing with θ in steps of 0.1.

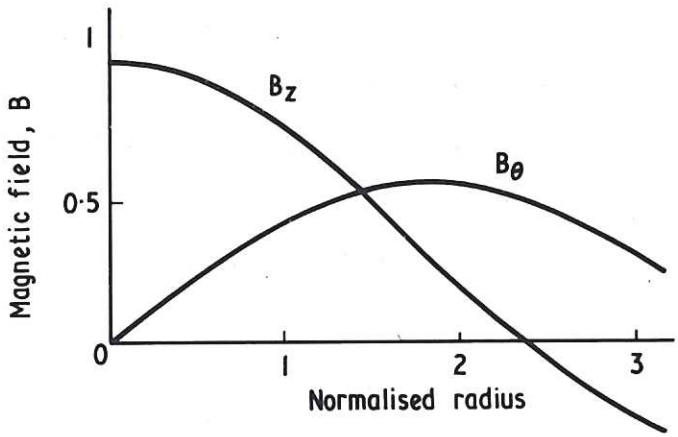

Fig.1b Radial distribution of magnetic fields in the BFM.

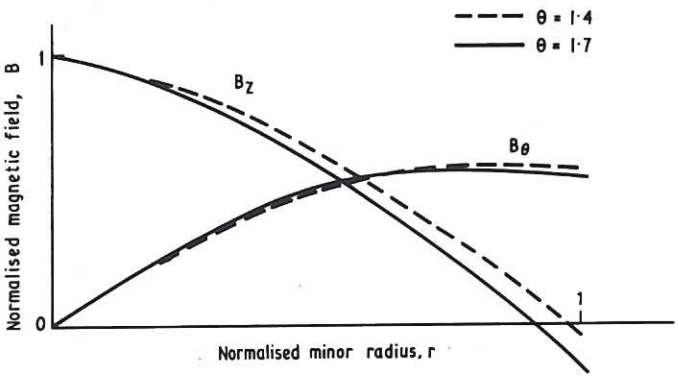

Fig.1c Radial distribution of magnetic fields in the HBM for two values of θ.

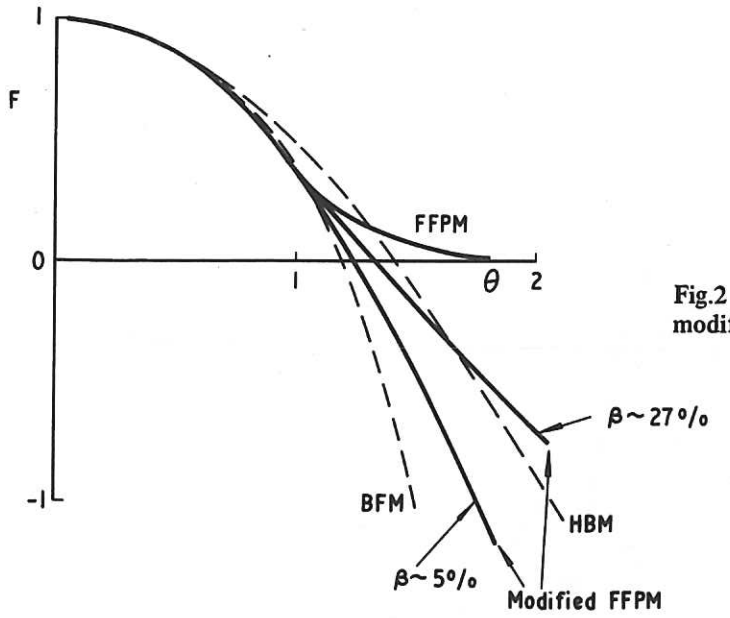

Fig.2 Reversal ratio vs pinch parameter for high beta modified paramagnetic models.

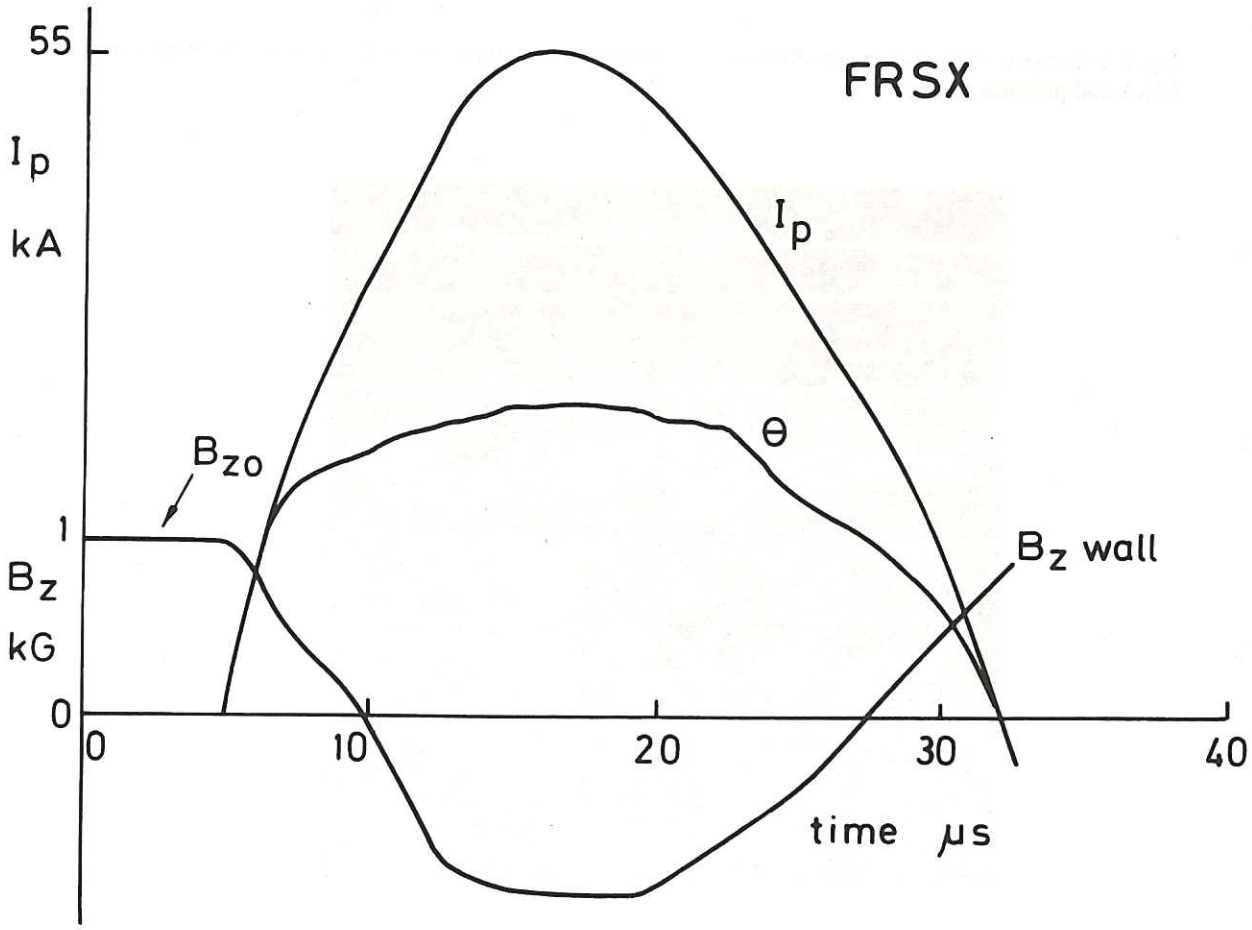

Fig.3 FRSX waveforms showing current I, toroidal field at wall B_{zWALL} and value of θ.

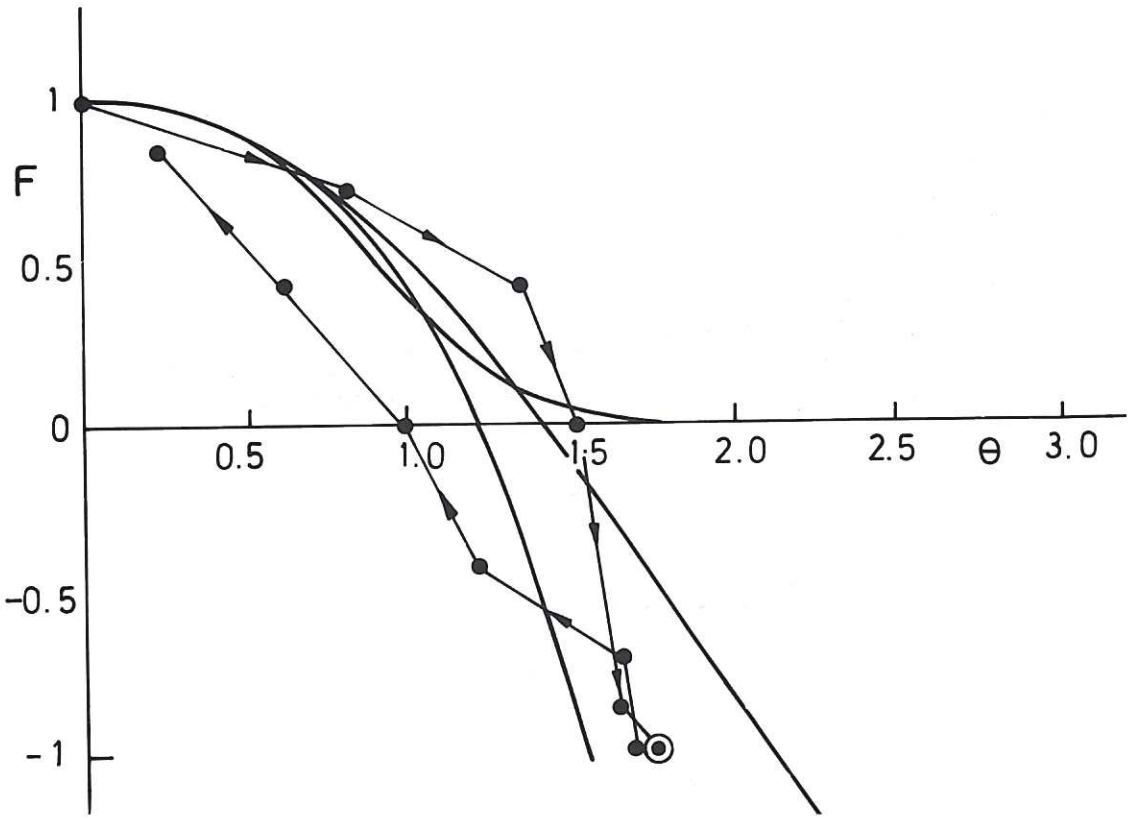

Fig.4 Trajectory of F–θ showing self reversal in FRSX. Data points are at 2.5 μs intervals. Peak current 55kA and pressure 40mtorr.

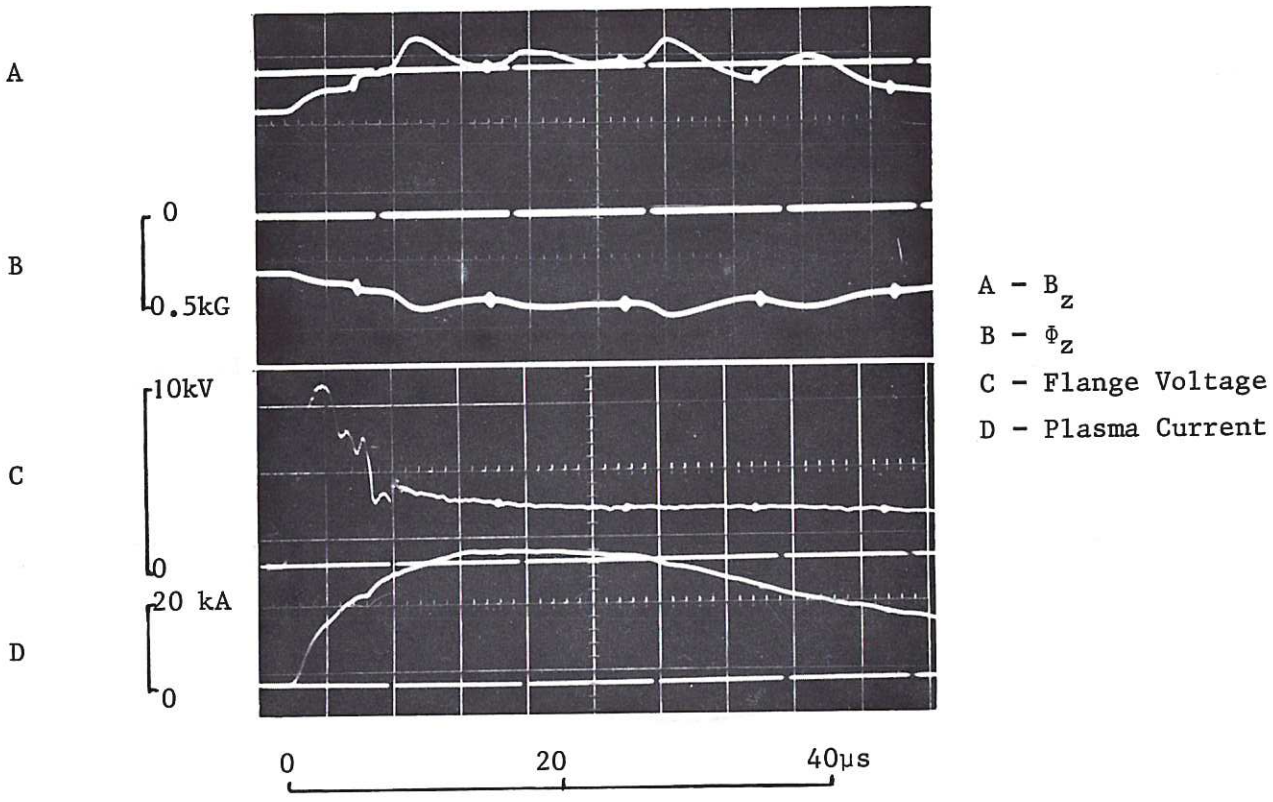

Fig.5 FRSX power crowbar waveforms showing relaxation and regeneration of the reversal. (A) B_{ZWALL}, (B) ϕ_z, (C) V_z flange voltage, (D) Plasma current.

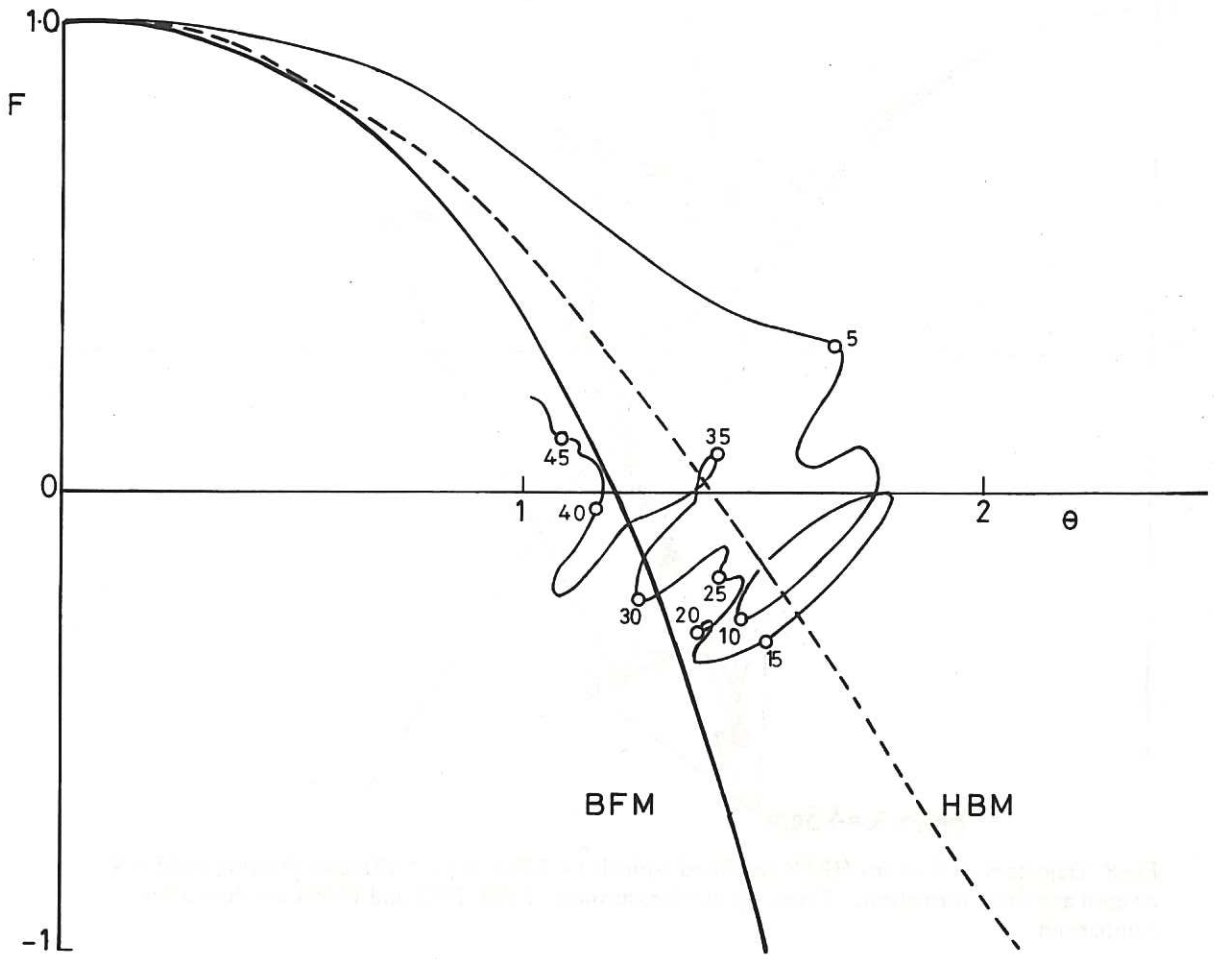

Fig.6 Trajectory of F–θ for FRSX power crowbarred discharge. HBM and BFM are shown for comparison.

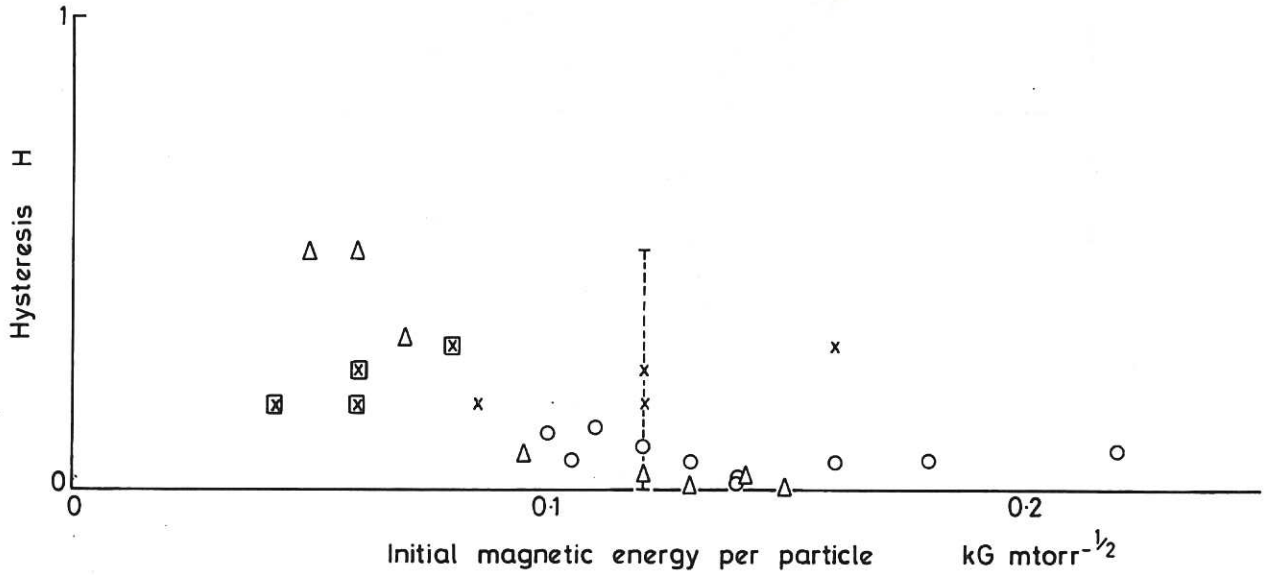

Fig.7 Variation of hysterisis, H, on FRSX with initial toroidal field, B_{ZO} and pressure.

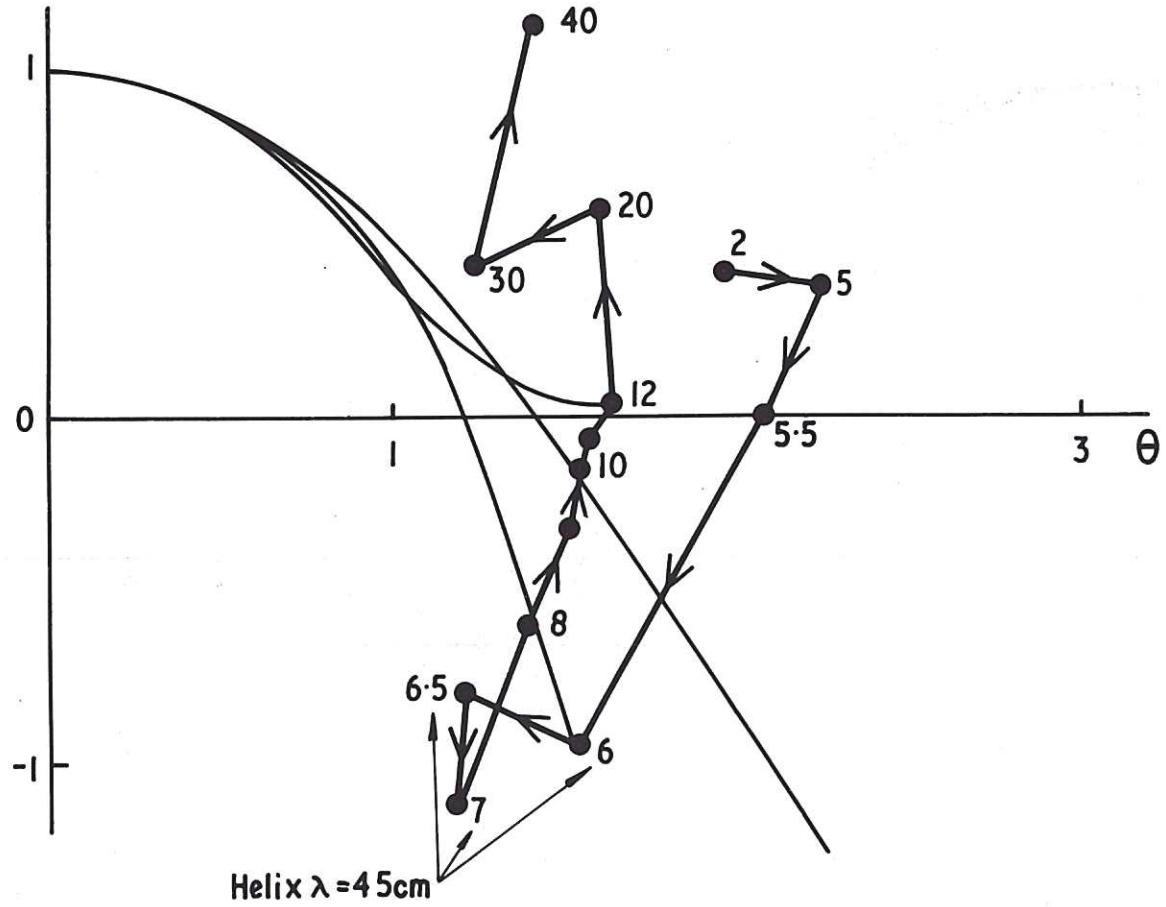

Fig.8 Trajectory of F–θ for HBTX stabilised z-pinch $\hat{I}$ = 75kA at p_o = 40mtorr showing rapid self reversal and helix formation. Times are in microseconds. HBM, BFM and FFPM are shown for comparison.

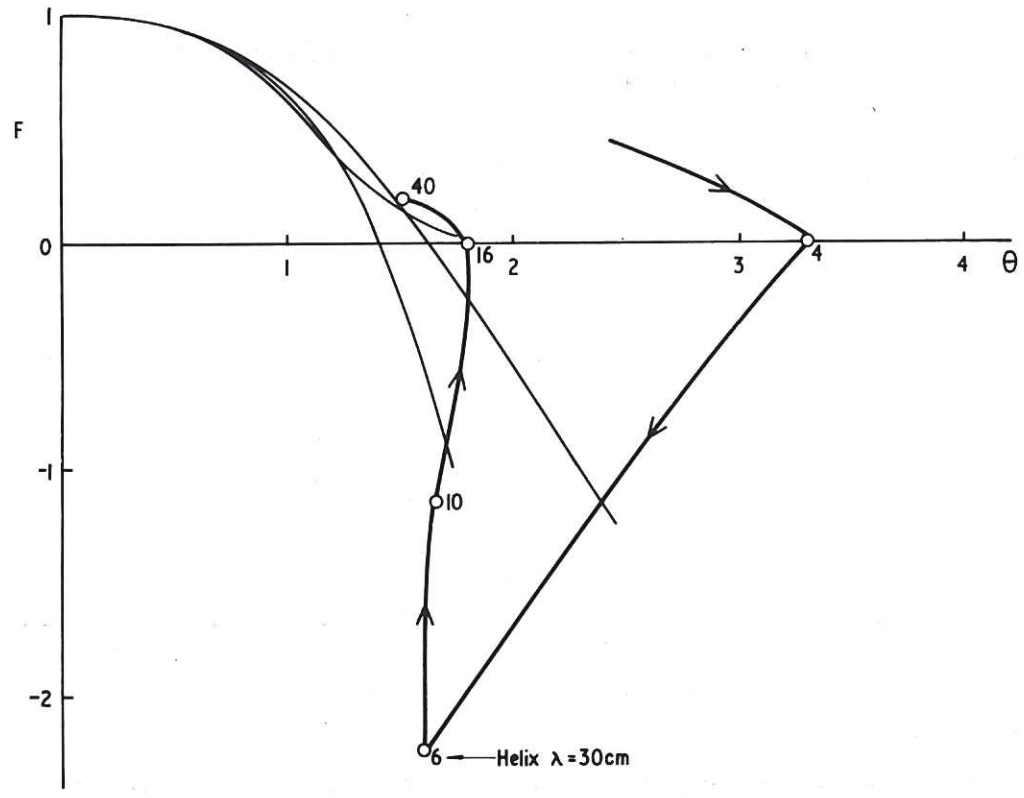

Fig.9 Trajectory of F–θ for HBTX stabilised z-pinch $\hat{I}$ = 100kA at p_o = 40mtorr. Times in microseconds. HBM, BFM and FFPM are shown for comparison.

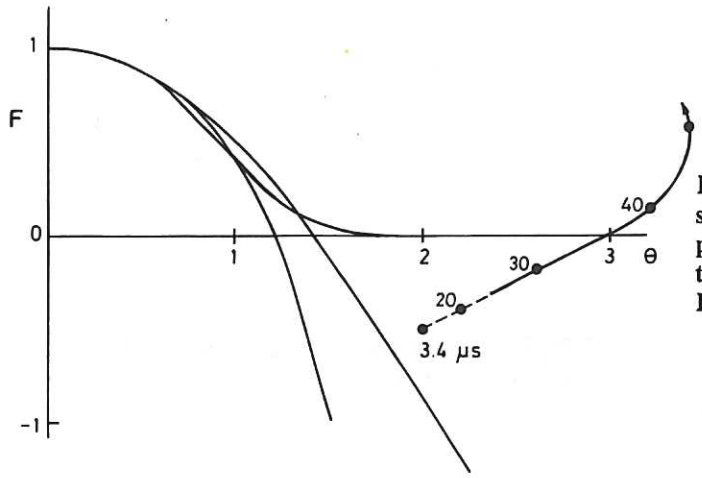

Fig.10 Trajectory of F–θ for HBTX fast programmed stable reversed field pinch with $\hat{I}$ = 40kA and p_o = 40mtorr, from peak current. At each point the time in microseconds is shown. HBM, BFM and FFPM are shown for comparison.

Fig.11 Trajectory of F–θ for HBTX reversed field pinch fast programmed to high θ at $\hat{I}$ = 75kA and p_o = 40mtorr showing double relaxation. Times in microseconds. HBM, BFM and FFPM are shown for comparison.

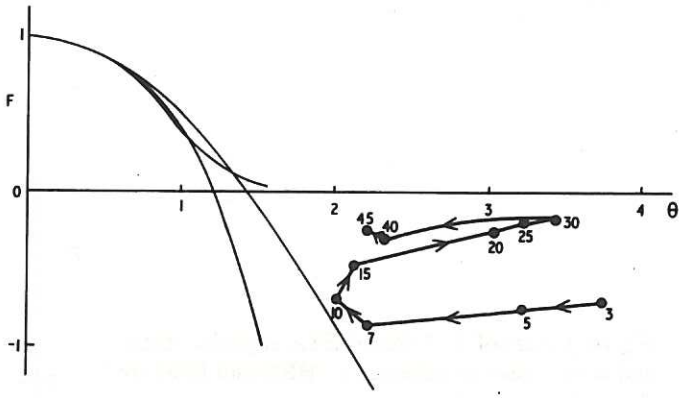

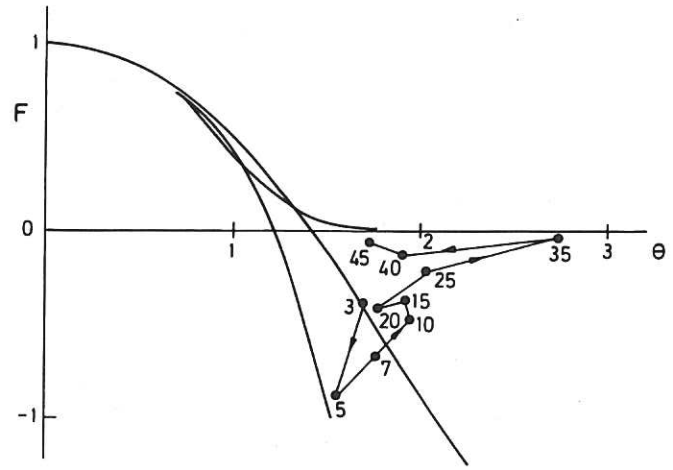

Fig.12 Trajectory of F–θ for HBTX high current stable reversed field pinch. Times in microseconds. HBM, BFM and FFPM are shown for comparison.

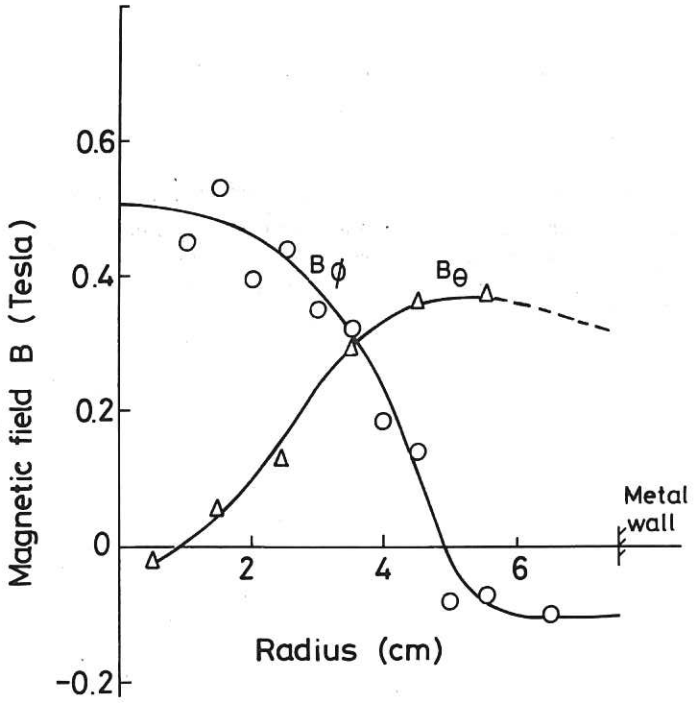

Fig.13 Magnetic field configuration of HBTX pinch after self reversal.

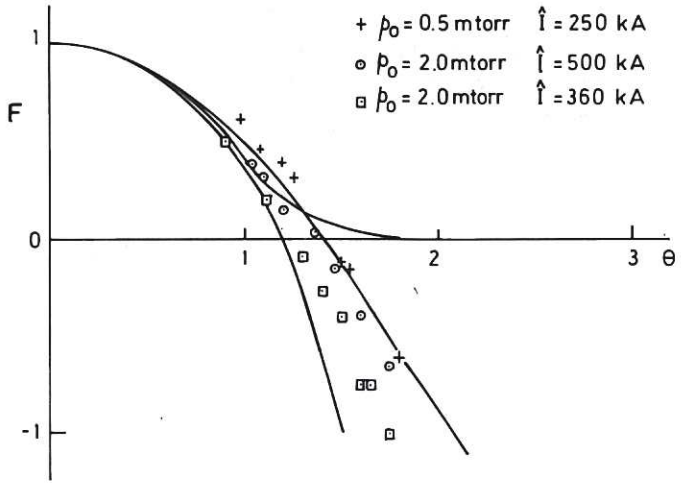

Fig.14 Values of F–θ from ZETA at peak current and at the onset of quiescence. HBM and BFM are shown for comparison.

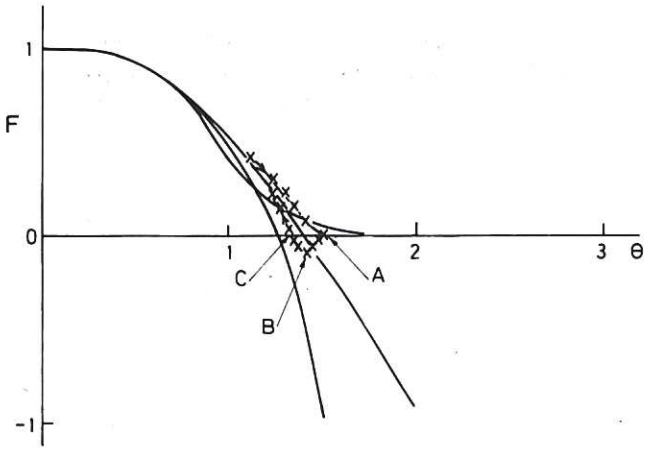

Fig.15 Trajectory of F–θ for ZETA (data at 0.2 ms intervals) for $\hat{I}$ = 0.81 MA, p_0 = 2.8 mtorr. The point A is at peak current, B is at the onset of quiescence and C at the end of quiescence.

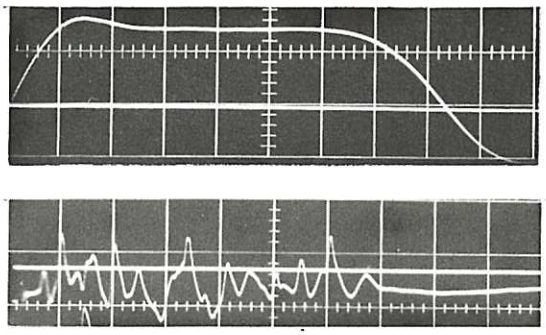

Fig.16 Oscillograms from the 3.5 linear pinch (a) plasma current $\hat{I} \sim 25$kA, (b) B_{zWALL} with $B_{zo} = 0.16$kG : Timescale 20μs/div.

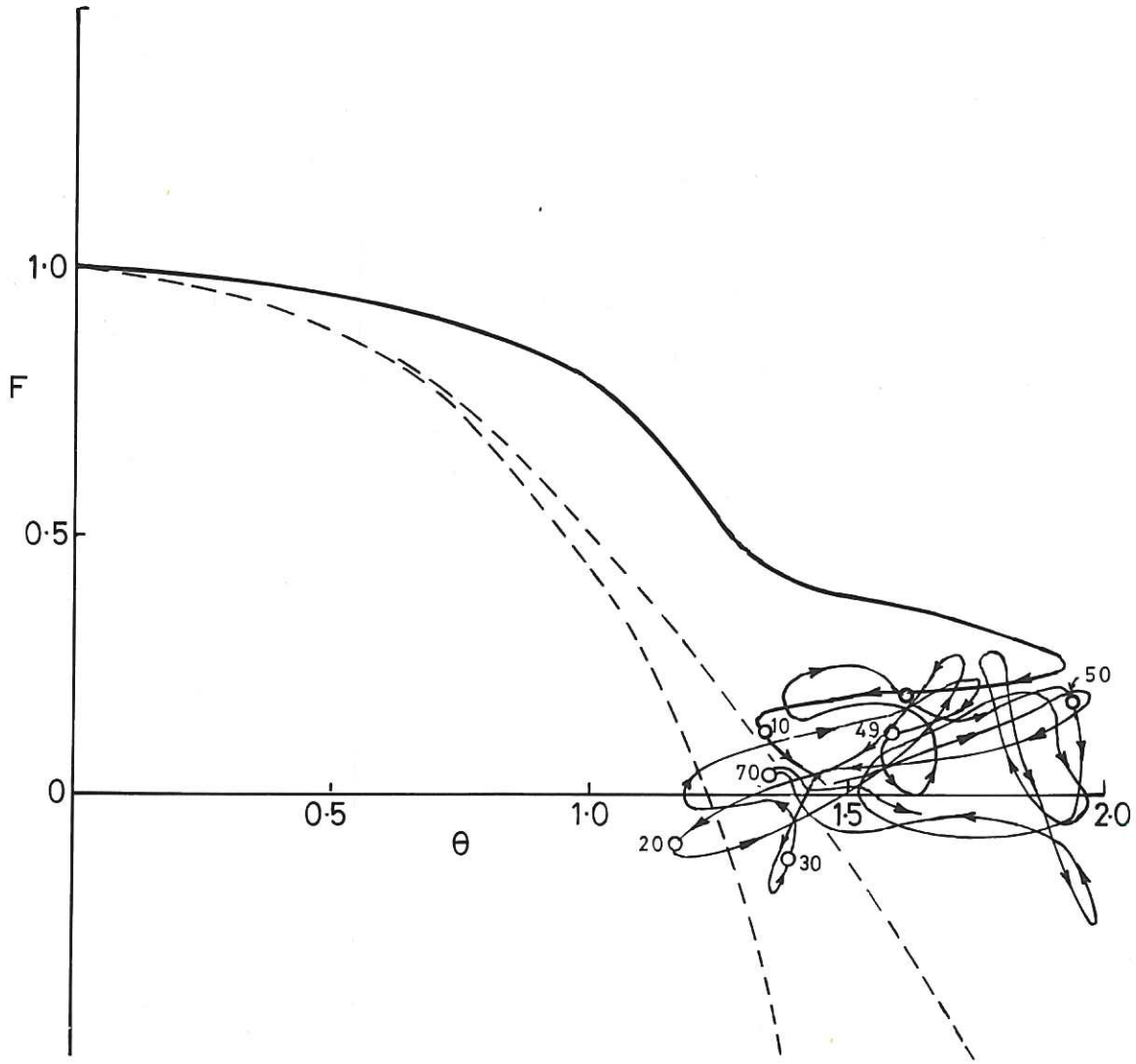

Fig.17 Trajectory of F–θ for the 3.5m linear pinch. HBM and BFM are shown for comparison.

HER MAJESTY'S STATIONERY OFFICE

Government Bookshops

49 High Holborn, London WC1V 6HB
13a Castle Street, Edinburgh EH2 3AR
41 The Hayes, Cardiff CF1 1JW
Brazennose Street, Manchester M60 8AS
Wine Street, Bristol BS1 2BQ
258 Broad Street, Birmingham B1 2HE
80 Chichester Street, Belfast BT1 4JY

Government publications are also available through booksellers